U.S. flood risk in the Anthropocene

Oliver Wing (oliver.wing@bristol.ac.uk)
University of Bristol https://orcid.org/0000-0001-7515-6550
William Lehman
US Army Corps of Engineers
Paul Bates
University of Bristol https://orcid.org/0000-0001-9192-9963
Chris Sampson
Fathom https://orcid.org/0000-0003-4094-2724
Niall Quinn
Fathom
Andy Smith
Fathom
Jeffrey Neal
University of Bristol
Jeremy Porter
First Street Foundation
Carolyn Kousky
University of Pennsylvania

Article

Keywords: flood risk estimates, hydrology, flood mitigation

Posted Date: June 14th, 2021

DOI: https://doi.org/10.21203/rs.3.rs-464320/v1

Abstract

A national depiction of high-resolution flood risk estimates has previously been thought to be beyond the grasp of reasonable computational capabilities. However, recent developments in inundation modelling now permit the first comprehensive national flood risk assessment of the US, which indicates an expected annual direct damage to property of 27 billion USD in 2020's climate. Current flood risk is disproportionately borne by poorer and more White communities, and is concentrated on the Atlantic and Gulf coasts, the Northeast through Appalachia, and the Pacific Northwest. Under a medium-case concentration pathway (RCP4.5), we project a 37% increase in risk by 2050 due to climate change alone. This climate signal appears to disproportionately impact Black communities, with risk increases concentrated again on the Atlantic and Gulf coasts. Medium-case (SSP2) projections of population change cause flood risk increases that dwarf the impact of climate change by 4:1, illustrating the need for a holistic view on changes in risk with consideration of all its constituent causes. These results make clear the desperate need for adaptation to flood and emergent climate risks in the US, with mitigation required to prevent acceleration of this risk into the latter half of the century. These results can and should inform zoning, regulations, and targeted adaptation policies, as well as motivate wide reaching reforms in how flood risk and emergencies are managed.

Main

The present means by which flood risk is managed globally is predicated on the assumption that history is a good predictor of the future. Be it enforcing regulations within flood zones defined using historical water level records, modelling the cost-benefit ratio of mitigatory actions based on historical flood probabilities, or not considering future risk when permitting new development, ubiquitous flood risk management tools fail to recognise that the nature of floods is changing.

Simple physical reasoning, complex physical modelling, and the recent observational record all suggest that a warming climate is intensifying the hydrological cycle, making extreme precipitation – and thus potentially inland flooding – more severe.[1–4] Equally, these sources agree that rising temperatures, leading to oceanic thermal expansion and ice mass loss, induce a rise in global sea levels.[5,6] This resultant coastal flooding may be further exacerbated by the low atmospheric pressure and high winds of storms, which themselves may intensify in the future.[7]

Flood hazard models simulate the physical characteristics of the inundation response to such flood drivers in order to identify potential flood risks. Typical models used for regulatory or commercial applications use historical observations (such as rainfall, river flows, or coastal water levels) as their driving input. Not only does the characterisation of these historical models as 'present-day' gradually become more indefensible with the passage of time, they are also instantly outdated if they fail to account for any of the ~1°C temperature rise already experienced during the industrial era, particularly in recent decades.[8] Flood risk management requires long term planning. It may be unwise to permit presently low-risk developments to occur in areas where climatic changes in the coming decades may

further heighten the flood risk. Investors and mortgage lenders also need to understand an asset's flood risk through the life of a loan or investment, possibly decades into the future. There is thus a latent need for flood risk assessments in common practice to account for existing and projected climatic non-stationarities.

Academic efforts to model flooding under climate change are in their infancy and so are rarely used for commercial or regulatory applications. Existing models can be broadly characterised as: (i) having spatial resolutions too crude to estimate property-level flood risk;[9,10] (ii) unrealistically modelling inundation with simplified volume spreading and storage algorithms;[11–13] (iii) lacking crucial local flood adaptation information;[14,15] (iv) directly employing precipitation inputs from general circulation models which are too coarse to represent extreme rainfall or resolve tropical cyclones;[16,17] (v) focussing on single flood drivers in isolation (e.g. riverine,[10] sea level rise,[13] storm surge[7]); and (vi) relatively limited evidence to support an understanding of the fidelity of their model output.[18–20]

Local-scale studies commonly ameliorate the above concerns relating to modelling accuracy. Flood mapping carried out by the U.S. Federal Emergency Management Agency (FEMA) is often based upon high-precision terrain data, fully surveyed river channels, local gauge information, and a full appraisal of local protection measures. While this represents the current gold standard approach for understanding flood hazard locally, the resource and labour required to replicate these methods at a continental scale is formidable. Consequently, since the start of a national flood mapping programme in 1967, only one-third of U.S. rivers have been modelled by FEMA and only one-quarter of these models have been updated in the last 5 years.[21] Furthermore, FEMA models are not mandated to account for climate change and simulate a limited number of flood frequencies, prohibiting a calculation of annualised flood losses. Thus, although policy requirements in the U.S. Water Resources Council's *Principles and Guidelines* of 1983 have illustrated the need for considering the future condition in flood risk management for the past four decades,[22] the state of the practice has not provided a consistent application of this on a national scale.

The recent work of Bates *et al.*[23] addresses the limitations of existing flood models in the US, fusing the accuracy of local studies with the spatial continuity of large-scale models. They present a hydrodynamic flood model at 30 m spatial resolution accounting for all major flood drivers and built with a well-documented flood protection database. The present and future impact of sea level rise, tropical cyclones, and changing weather patterns are all explicitly represented. Crucially, they benchmark their model against high-quality local flood maps, flood claims information, and, in Wing *et al.*,[24] observations of real flood events. These validation exercises determined the skill of the Bates *et al.* US-wide flood model to be approaching that of local studies and historical observations (80–90% flood extent similarity), while providing a consistent and comprehensive picture of flood hazard spatially. Bates *et al.* focus exclusively on the flood hazard; however, their hazard model uniquely enables us to quantify present and future U.S. flood risk – the financial and human implications of the physical phenomenon – with wider scope, scale, and fidelity than prior research.

Risk assessment requires a quantification of the hazard (local flood intensities and frequencies), the exposure (the location and characteristics of buildings, people, and businesses), and vulnerability (the extent to which hazard intensity impacts exposed entities). For the latter two constituents of risk, we employ detailed information from the U.S. government. The National Structure Inventory (NSI), a database of building locations and characteristics for residential and non-residential structures, was utilised for the representation of exposure. U.S. Army Corps of Engineers (USACE) depth-damage functions are utilised to describe the vulnerability of these buildings to flooding. Combining these three components (hazard, exposure, and vulnerability) yields a step-change in understanding of U.S. flood risk by providing the first national-scale flood risk assessment using property-level residential and non-residential asset data alongside spatially complete hazards maps of multiple frequencies (see Methods for further details). Estimates of annualised flood losses are compared to those recorded historically, and while we do not expect to replicate these precisely owing to uncertainties in those observations and their questionable relevance to present conditions (both in terms of hazard frequency and exposure availability), we use the comparison to demonstrate that the risk model provides sensible quantifications at the U.S. scale (see Supplementary Information).

This analysis reveals that annualised U.S. flood losses are currently $27.4 billion on average and are projected to rise to $37.5 billion by 2050 under the RCP4.5 scenario. This is a 36.7% increase across a typical 30-year mortgage term commencing today: near-term impacts which are essentially locked-in climatically; that is, these projections hold even if dramatic decarbonization is undertaken immediately.

In Fig. 1a, we can see the distribution of AAL by U.S. county. Intuitive hotspots are found in highly populated counties along both coasts, as well as across the Northeast and through Appalachia. Controlling for exposure (i.e., the total value of what could potentially be damaged) in Fig. 1b, hotspots emerge in coastal Louisiana, Appalachia and the inland Northeast, and rural counties of the Pacific Northwest and Northern California. While many of these counties do not have high absolute annual losses, they are proportionally high-risk with AALs greater than 0.2% of exposure (losses expressed as a proportion of total value). Climatic changes alone cause dramatic increases in risk along the east coast in counties which are already high-risk (Fig. 1c and 1d). The intensification of hurricanes on the east coast is particularly evident in risk changes, principally a result of greenhouse gas emissions weakening vertical wind shear in the North Atlantic and permitting hurricanes to intensify more than usual.[25] The impact of these projected changes to hurricane behaviour on coastal surges are most keenly felt in Virginia, the Carolinas, and the west coast of Florida, while the contribution of sea level rise to future coastal floods dominates the remaining stretches of the Atlantic and Gulf coasts.[23] Intensifying rainfall, both hurricane and non-hurricane, is also expected to drive up risk in inland counties of Florida and the Northeast. Climate risk hotspots are further found in some already-risky western counties in California, Oregon, and Washington. Conspicuous by their absence are risk hotspots along the Mississippi-Missouri, perhaps due to lower asset values and the dominant land-use being agricultural. Furthermore, climate change impacts for large river systems are highly uncertain, while clearer positive signals emerge for short-duration rainfall and sea level rise.

The FEMA Special Flood Hazard Area (SFHA), determined by the nationwide patchwork of local-scale FEMA flood models, is the *de facto* flood risk zone in the U.S.[26] A number of regulations apply to development within SFHAs, as well as the mandatory purchase of flood insurance for those with a federally backed mortgage. Though it was not designed to be a risk communication product, it has become synonymous with that in the public view. Properties located outside the SFHA are commonly misconceived to be risk free, when, in reality, there may simply not be an up-to-date local flood map, they may be at risk of unmapped pluvial (or, indeed, fluvial) floods, or they may be outside of the 100-year flood zone where lower frequency floods can still occur. Additionally, for those located in the 100-year floodplain (at least a 1% chance of inundation each year), their recurrence of flooding can be anywhere from every other year to once every hundred years on average, and these varying probabilities have dramatically different outcomes in the evaluation of risk. The frequency of floods outside the SFHA and its discontinuous spatial coverage has been well documented elsewhere,[21,27,28] but here we demonstrate that less than half of the nation's flood risk is located within the SFHA. Properties within the SFHA are currently subject to AALs of $13.0 billion (47.6%), while AALs outside total $14.4 billion (52.4%). Proportional risk is much higher in the SFHA, with an AAL equal to 0.399% of exposure; roughly 20 times the relative risk of non-SFHA properties (0.021%). This is illustrative of the large number of low- or no-risk buildings outside the SFHA, yet it still remains that the majority of U.S. flood risk is unmapped by FEMA. Climate-induced risk changes in the SFHA are expected to be more intense than elsewhere. Within-SFHA AALs are projected to rise by 42.5% to $18.6 billion (or 0.568% of exposure) by 2050, while the outside-SFHA increase is projected to be 31.5% to $18.9 billion (0.027%).

Flood risk is not borne equally by all. We use census-tract level data from the 2019 American Community Survey to assess the demographic characteristics of flood risk across the US. Normalising for exposure (to understand risk as a fraction of the total that could be damaged), we consistently see that present-day flood risk is concentrated in both the most White and the most impoverished communities across the nation (Fig. 2a). When grouped into ordinal quintiles (bins containing 20% of U.S. census tracts), the data indicate a persistent increase in relative AAL with increasing poverty rate and the proportion of the population that is White. The flood risk of the top 20% proportionally White and impoverished census tracts (>90% White, >22% in poverty) is roughly 10 times higher than those which fall into the least White and the least impoverished quintiles (<30% White, <5% in poverty). The spatial distribution of these census tract groups and their relative risk is shown in Fig. 3a and 3b. More White and impoverished communities with high relative risk are noticeably concentrated in Appalachia (West Virginia and Kentucky; Fig. 3ai), covering the high-risk counties highlighted in Fig. 2b. Rural and small-town Pennsylvania, other communities in the Ohio River valley (Fig. 3aiv), as well as northern New England (Fig. 3aii) and Oregon lie at the nexus of high-risk, high-poverty, high-White proportion. The relative risk of the opposite group – census tracts with the smallest White population proportions and lowest poverty rates – is shown in Fig. 3b. These low-risk communities are predominantly urban, with clusters on both coasts of the US. Suburbs of Washington, D.C. (Fig. 3bi), and a stretch of tracts from Philadelphia, PA through New York City, NY (Fig. 3bii) generally have low relative flood risk, with AALs less than 0.01% of exposure. In California, communities in Los Angeles (Fig. 3biii), San Francisco (Fig. 3biv), and a handful

in the Central Valley are also generally more affluent, less White, and lower risk. Pockets of urban centres in the Deep South also share these traits: Montgomery and Birmingham, AL; Atlanta, GA; Tallahassee, FL; and Houston, San Antonio, and Dallas, TX.

Meanwhile, expected changes in flood risk up to 2050 show largely the opposite trend in demography compared to who bears present-day risk. The sensitivity of flood risk to climate change is concentrated in Black communities across the US. Fig. 2b, with census tracts again grouped into equal-count quintiles of Black population proportion, illustrates that the more Black an area is, the larger its expected increase in flood risk due to climate change. The top 20% proportionally Black census tracts (>20% Black) are expected to see flood risk increase at double the rate of the bottom 20% (<1% Black) of Black census tracts. Fig. 3c illustrates that areas with high Black population proportions are clearly concentrated across the Deep South, in the very locations where climate change is expected to intensify flood risk (Fig. 2c). Urban and rural areas alike from Texas through Florida to Virginia contain predominantly Black communities projected to see at least a 20% increase in flood risk over the next 30 years. Indeed, virtually every high-Black population proportion census tract in urban areas of Florida, Alabama, Georgia, Louisiana, Mississippi, and the Carolinas (Fig. 3ci and 3civ) bear outsized climate risks. The same can be said for Black communities in Detroit, MI; Cincinnati, Dayton, Columbus, and Cleveland, OH (Fig. 3cii); as well as those around the Chesapeake Bay (Fig. 3ciii). In contrast, most census tracts with the lowest Black population proportions see very little increase in climate-induced flood risk (Fig. 3d): particularly in the predominantly White central U.S. and Midwest (Fig. 3di and 3dii) and the low-Black populations of the arid Southwest (Fig. 3div). Some communities with a low proportion of Blacks in the Northwest see heightened future risk proportionally, but these are mostly small in magnitude due to their current low risk (Fig. 3diii). Present and future trends in the flood risk of other demographic groups are less clear and consistent and are shown in Supplementary Figs. 1-9.

Climate will not be the only thing changing over the next 30 years. The U.S. population is expected to continue to grow, and so, accordingly, is development. We use gridded maps of population from the U.S. Environmental Protection Agency (EPA) to calculate the current population exposed to floods, and their gridded projections of 2050 populations under the SSP2 scenario to analyse the relative contributions of climate change and population growth to future U.S. flood risk (Fig. 4a). The average annual exposure (AAE) of the current U.S. population to flooding is 3.63 million (1.18%). Climate change is projected to increase the AAE of present populations to 4.31 million (1.41%); an increase of 18.6%. Meanwhile, population growth alone in a static climate (i.e., no future changes in flood hazard) would result in a 72.6% increase to 6.27 million AAE by 2050. This corresponds to 1.60% of 2050's projected population, indicating that future development is projected to disproportionately intensify in hazardous areas (given the present-day proportion is 1.18%). Absent of policies to direct new development into safer areas, the contribution of population growth to future U.S. flood risk dwarfs that of climatic changes. Population growth alone accounts for 74.7% of the increase in AAE to 2050, while climate change represents 19.1% of the change. There is a remaining 6.2% (yellow in Fig. 4a) of 2050's projected AAE which represents the intersection of both climate change and population growth. Conceptually, this is due to floods intensifying in places where populations are also increasing – and so the compound intensification of

both hazard and exposure is required to capture the increased total risk. AAE of the U.S. population to floods in 2050 is projected to be 7.16 million (1.83%), a 97.3% increase from the present-day.

Fig. 4b, like Fig. 1a, shows that concentrations of population AAE generally fall within populous U.S. states. Populations of 547k, 345k, 247k, and 247k in Florida, California, New York, and Texas respectively are expected to be impacted by flooding every year, on average, under current conditions. Fig. 4c shows that, proportionally, West Virginia, Vermont, Florida, and Louisiana have the highest AAEs: they can expect over 2% of their populations to be impacted by flooding every year currently (mirroring Fig. 1b). AAE increases due to climate change are generally found across the east coast, with existing Texas and Florida residents seeing a roughly 50% increase in flood exposure by 2050 (Fig. 4d). Interestingly, AAE increases due to population growth occur in many places where increases due to climate change are minimal (Fig. 4e). Intensification of development on existing floodplains is relatively severe in the currently sparsely populated central Prairie States and the Deep South. The consequence is a more widespread increase in flood risk to 2050 than Fig. 1 suggests: states with little climate risk may still see large increases in flood risk unless future development patterns are managed appropriately (Fig. 4g). Areas where the compound effect of climate change and population growth is significant are scattered across the nation: over 10% of the risk increase to 2050 is compound in West Virginia, Louisiana, Idaho, and Mississippi (Fig. 4f).

With future development patterns projected to be 4x more impactful than climate change in elevating national flood losses, the importance of improved flood risk management in the U.S. is clear. More aggressive local land use controls restricting new developments in the highest risk areas, coupled with stronger building codes, could help lower the growth in flood losses that is currently projected to accompany expanding populations. Such regulations imposed on future development will also need to be accompanied by investments in both relocation and retrofits for existing construction in areas where flood risk is high and/or growing. The federal government has several programs that currently fund such efforts, although not at levels that will be required to fully adapt to increasing risk.[29] Further, several of these programs have been criticized for privileging more affluent and White communities.[30,31] Equity-centred reform in light of climate change is needed for U.S. disaster policy; a call given greater emphasis by the demographic make-up of present and future bearers of U.S. flood risk shown here.

An important conclusion from Bates *et al.* should not go neglected, however. They found that when considering flood hazard projections derived from only the central 50% of climate model ensemble members (i.e., ignoring outlier simulations), the variability between models representing the present-day is over double the magnitude of the change signal to 2050. In simpler terms, increased flooding due to climate change is within the error of present-day flood models. Furthermore, these projections assume no further adaptation to present and future flood risks take place. Existing protection measures maintain their integrity up to their original design standard, but no further defences are projected to account for increasing flood hazard or the proliferation of flood-exposed developments. While future work will examine the efficacy of targeted adaptation measures in drawing down the flood risks we project here, it is fair to assume that some level of adaptation will be put in place to protect new development. That

being said, the ability to understand future risk as the process of development takes place is essential to reducing risk in future environmental conditions.

The threat that floods presently pose – both direct and indirect, tangible and intangible – is evidence enough that there is a dearth of flood resilience in the U.S., regardless of what the future holds in terms of climate and demographic change. Layered on top of this already critical problem is the large increase in risk that we project a warming world would portend. These impacts are so near-term that climate mitigation (i.e., decarbonization) is futile, meaning we can only adapt to this increasing risk in areas currently developed. We thus have to adapt to both the 'now' and to the future. Mitigation will largely determine how much worse flood hazard will get in the latter half of this century. The lack of quality publicly available flood risk information has meant risky developments have proliferated across the U.S.; planning and investment decisions by the public, governments, and corporations rarely consider flood risk adequately.[32] The current state of the science means there is no longer an excuse for this to continue. It is critical that information on changing risks be made widely available and transparent in order to fully inform housing and mortgage markets to guide capital away from the riskiest areas. The findings of this paper provide important insights for communities and the federal government in designing future flood risk management interventions and in allocating federal dollars more effectively. Models such as these can and should inform zoning regulations to prevent anticipated future developments making largely inevitable hazard changes unnecessarily inflate risk. Adaptation policies can be targeted towards locations with disproportionate risk, or where risk is expected to increase, using these data. Furthermore, public consciousness surrounding present and future flood risks must improve to spur individual and collective risk reduction. To that end, these flood data have been released on FloodFactor.com to ensure every American resident has access to high-quality flood information.

Methods

Hazard model

The physical flood data used to calculate risk in this paper were published in Bates *et al.*,[23] itself an evolution of the first spatially continuous U.S. flood model presented by Wing *et al.*[20] and the global-scale modelling methods of Sampson *et al.*[33] In this section, the main methods and model validation studies are outlined. For more information, the reader is referred to Bates *et al.*[23]

The flood inundation model, at its core, solves the local inertial formulation of the shallow water equations in 2D (based on LISFLOOD-FP)[33,34] over a regularly spaced 1 arc second (~20–30 m in the US) grid. This formulation has been shown to produce indistinguishable answers to the full solution of the shallow water equations for typical flood inundation problems (i.e., subcritical flows), given typical input data errors.[33,35] Crucially, it provides these answers much faster than full solutions or other common simplifications of the shallow water equations (e.g., the diffusive wave)[36], owing to its linear scaling of stable time step with grid size.[33] Alongside vectorisation and parallelisation of code,[37] accurate

computational hydraulics can thus be deployed at high resolutions over large spatial domains with practicable runtimes. The set of return period hazard maps at 1 arc second resolution used in this analysis took ~2 months on a ~2000 core compute cluster.

The 1” grid is populated with elevation values principally obtained from the U.S. Geological Survey (USGS) National Elevation Dataset (NED). The NED consists of a plurality of high-accuracy LiDAR data, covering 39% of the contiguous U.S. land area and two-thirds of its population. The NED is further infilled by sub-national LiDAR terrain data where available.

River channels are represented in 1D, decoupled from the 2D grid to enable river channels of any size (including <1” width) to be modelled.[34] A flow accumulation grid was forged using the composite elevation data alongside the USGS National Hydrography Dataset, ensuring correct alignment of 1D channels with their 2D valleys. River bathymetry (particularly bed elevation) is mostly unobserved over large spatial domains, but since channels convey the bulk of flood flows the approximation of their bathymetric properties is essential. Channels are thus parameterised under the assumption that they can convey a certain return period discharge (generally the 2-year flow, rising to 5-year in arid regions), with their bed elevations thus estimated using an inverted gradually varied flow solver (which solves for water height rather than discharge).[38]

Return period discharges for channel bed estimation, and indeed for the extreme flows to simulate flooding are computed using a regional flood frequency analysis (RFFA) based on the methods of Smith *et al.*[39] and further extended in Bates *et al.*[23] This involved pooling almost 7000 USGS river gauges into proximal and hydrologically similar groups in order to compute an index flow for every cell on the flow accumulation array (with upstream area >50 km^2). Since flow records are generally too short to understand extreme flow behaviour, the RFFA substitutes time for space by again pooling hydrologically similar river gauges to derive growth curves. These curves define the proportional change to a given index flow to get a given return period flow. Bates *et al.* report a 6% and 29% error for 10- and 100-year flows, respectively, likely within observational error for gauge-based extremes.[40] In coupling channel conveyance to the RFFA, errors in flow estimation are implicitly dampened to some extent. If the RFFA overestimates flows at a given location, the channel will be larger to account for this, and vice versa.

Pluvial modelling is executed to simulate the flashier flood response on smaller headwater streams (<50 km^2 drainage area) and due to surface water flooding directly through a rain-on-grid approach. The boundary conditions take the form of Intensity-Duration-Frequency estimations from National Oceanographic and Atmospheric Administration (NOAA) Atlas 14. The maximum flood depth from 1-, 6-, and 12-hour pluvial simulations form the hazard map for each return period. River channels are explicitly represented in the pluvial simulations, allowing channels to convey water and drain floodplains during simulated extreme precipitation events.

To account for climate change, both up to 2020 and to 2050, we adopt a change factor approach. A large synthetic catalogue of hurricane events based on the methods of Emanuel *et al.*[41] and Feldmann *et al.*[42]

was simulated using 7 downscaled general circulation model (GCM) scenarios to yield 55,000 years of synthetic hurricanes for each time horizon. 55,000 annual maximum (AMAX) daily rainfall accumulations were then extracted. 21 GCM ensemble members from National Aeronautics and Space Administration (NASA) Earth Exchange Global Daily Downscaled Projections (NEX-GDDP) were used to create an equivalent 55,000 years of rainfall AMAXs via sampling from fitted Generalised Extreme Value (GEV) distributions. For each synthetic year, the maximum hurricane or NEX-GDDP AMAX was retained. Rainfall changes with respect to an historical baseline (1980-2000) simulation period were computed for the 2020 and 2050 climate states, based on Representative Concentration Pathway (RCP) 4.5. These changes directly perturb the historical pluvial IDF curves outlined above.

For the fluvial model, these rainfall time series were routed through calibrated HBV hydrological models for ~700 U.S. river catchments to generate 55,000 years of synthetic streamflows for historical, 2020, and 2050 climate states. Change factors with respect to the historical run were again computed and the regionalisation procedure outlined above (for the RFFA) iterates change factors for every U.S. river. Changes are then applied directly to each RFFA-derived return period flow.

For coastal modelling, the historical water levels from 68 detrended NOAA tide gauges (with hurricane events stripped out) were extracted and adjusted to 2020 mean sea levels based on Kopp *et al.*[5]. 55,000 years of synthetic non-hurricane extreme water levels were generated at each site, and the Global Tide and Surge Reanalysis was used to interpolate between them.[43] The pressure and wind fields from the above hurricane event sets were used to drive the GeoCLAW coastal flood model to produce 55,000 years of synthetic hurricane extreme water levels.[44] At coasts, flood inundation occurs due to the joint probabilities that riverine and oceanic flooding co-occur. Using the stochastic model of Quinn *et al.*,[45] we link the return periods of univariate hurricane and non-hurricane fluvial and coastal floods to the return period of the synthetic multivariate event. Flood inundation maps at coasts thus represent the compound impact of fluvial and coastal floods at each return period.

Flood defences are represented in a variety of ways, wrought from a painstaking scouring of national and sub-national databases of flood adaptations across the US. Levees from the USACE National Levee Database, as well as other projects identified locally, were incorporated explicitly into the model. The function of dams from the USACE National Inventory of Dams was used to adjust the bankfull return periods of channels. Other grey, green, and coastal adaptations were also incorporated. See Bates *et al.*[23] for further details.

Bates *et al.* carried out a number of model validation exercises for the predicted physical hazard. They compared the model to high-quality FEMA flood maps, where they exist, finding 78% similarity between these local-scale engineering models and the large-scale flood model, rising to 82% in coastal regions. Given typical errors associated with flood modelling at any scale, Bates *et al.* refer to this degree of similarity as within error. This test of the modelled 100-year flood was repeated for the 100-year flood maps generated by the Iowa Flood Center, finding 87% similarity to these higher-accuracy models. For the 5-year flood – more difficult to model owing to its modest size and thus sensitivity to channel

parameterisation and microtopography – the similarity between Bates *et al.* and the Iowa Flood Center was 69%. Wing *et al.*[24] furthered the validation of the Bates *et al.* model by simulating historical flood events and comparing them to observations. They found roughly 87% similarity between modelled inundation and observations, and a mean bias of 0.17 m compared to observed flood depths. These studies thus demonstrate the fitness for purpose of the Bates *et al.* hazard model in a national-scale risk calculation framework.

Building data

The National Structure Inventory (NSI) defined the exposure in this assessment. The NSI is a database developed by the USACE to support their dam and levee safety programs, as well as real time consequence assessments and planning functions for risk mitigation. The NSI is designed to represent every structure in the United States as a point, as accurately placed and attributed as possible. The product is described in more detail in USACE documentation.[46] This study used the updated NSI V2 which is restricted by a license, therefore no results are shown below the census block level. This version of the NSI was developed in 2019 by coordinating many datasets such as the Microsoft building footprints layer, the CoreLogic parcel database, ESRI business layer, Census data, and many other datasets to derive a best-of-breed inventory fit for evaluating natural disasters. The inventory is described by occupancy types, which are linked to standard depth-damage relationships to understand their vulnerability to flooding. Valuations are based on a variety of sources and are designed to represent depreciated replacement value.

Population data

The U.S. EPA EnviroAtlas programme produced a 30 m resolution dasymetric map of contiguous U.S. populations, which we intersected with the multi-frequency hazard data to estimate average annual flood exposure. The EPA data were generated via reallocating 2010 U.S. census block populations to 30 m cells based on maps of land cover and slope. The projections of future populations are drawn directly from the U.S. EPA Integrated Climate and Land-Use Scenarios (ICLUS) projections.[47] This involves the use of a 90 m resolution spatial allocation model to assign county-level population change estimates (from a demographic model) to housing units. Fertility, mortality, and migration are the key variables of the demographic model, used to project county-level cohorts split by gender, ethnicity, and age. Datasets from population, housing units, and non-residential land-use, to groundwater availability and transport infrastructure form inputs to the spatial allocation model, which requires parameters such as household size, land-use demand, and travel times to downscale county-level populations to the 90 m grid. Given the use of the RCP4.5 climate scenario, we employ the complementary Shared Socio-economic Pathway (SSP) 2 projection of demographic change. This represents a medium-growth scenario, following U.S. Census Bureau projections of the contiguous U.S. growing to almost 400M people by 2050. Models of socio-economic change are commonly laden with assumptions; for instance, the continuation of historical trends in migration patterns, land-use change, and demand for transport and amenities. The data used thus represent a single plausible population projection, out of many possibilities, based on

historically-derived model parameters. As such, these projections of change are highly uncertain, not least since they are predicated upon the continuation of historical development patterns and how growing populations consume and interact with impervious surfaces. However, conclusions drawn with these data are aggregated to the state and national level, where likely substantial local uncertainties will, to some extent, cancel each other out. The results demonstrate that plausible patterns of future development are the overwhelming driver of increased flood risk, which, in spite of projection uncertainty, are conclusions which cannot be ignored. For more information, the reader is referred to U.S. EPA report.[47]

Vulnerability functions

The vulnerability functions utilized for this report were sourced from a curated database developed to support a variety of the USACE Hydrologic Engineering Center's flood risk modelling activities. The residential damage functions represent those required by policy – Economic Guidance Memorandum (EGM) 01-03 and EGM 04-01 – for use by USACE.[48,49] Non-residential functions are selected from the HAZUS database from previous USACE projects, based largely on expert elicitation.[50] These are shown in Table 1.

Occupancy Type	Source	Description
RES1-1SNB	EGM	One floor, no basement
RES1-1SWB	EGM	One floor, with basement
RES1-2SNB	EGM	Two floors, no basement
RES1-2SWB	EGM	Two floors, with basement
RES1-SLNB	EGM	Split level, no basement
RES1-SLWB	EGM	Split level, with basement
RES2	FIA	Mobile home
RES3AI	USACE - Galveston	Condominium, living area on multiple floors
RES3BI	USACE - Galveston	Condominium, living area on multiple floors
RES3CI	USACE - Galveston	Condominium, living area on multiple floors
RES3DI	USACE - Galveston	Condominium, living area on multiple floors
RES3EI	USACE - Galveston	Condominium, living area on multiple floors
RES3FI	USACE - Galveston	Condominium, living area on multiple floors
RES4	USACE - Galveston	Average hotel/motel
RES5	USACE - Galveston	Average institutional dormitory
RES6	USACE - Galveston	Nursing Home
COM1	USACE - Galveston	Average retail trade
COM2	USACE - Galveston	Average wholesale trade
COM3	USACE - Galveston	Average personal/repair services
COM4	USACE - Galveston	Average Prof/Tech services
COM5	USACE - Galveston	Bank
COM6	USACE - Galveston	Hospital
COM7	USACE - Galveston	Average Medical Office/Clinic
COM8	USACE - Galveston	Average Entertainment/Recreation
COM9	USACE - Galveston	Theater
COM10	USACE - Galveston	Garage
IND1	USACE - Galveston	Average Heavy Industrial
IND2	USACE - Galveston	Average Light Industrial
IND3	USACE - Galveston	Average Food/Drugs/Chemicals
IND4	USACE - Galveston	Average Metals/Minerals Processing
IND5	USACE - Galveston	Average High Technology
IND6	USACE - Galveston	Average Construction
AGR1	USACE - Galveston	Average Agriculture
REL1	USACE - Galveston	Church
GOV1	USACE - Galveston	Average Govt Services
GOV2	USACE - Galveston	Average emergency response

EDU1	USACE - Galveston	Average School
EDU2	USACE - Galveston	Average College/University

Table 1. The provenance of the depth-damage functions applied in this analysis.

Wing *et al.*[51] posit that vulnerability functions are an underappreciated source of uncertainty in risk modelling, principally due to a lack of data with which to characterise the relationship between hydrological variables (e.g. water depth) and their consequences (e.g. building damage). They found the residential depth-damage curves used in this analysis matched poorly with empirical data contained in the NFIP claims record, which illustrated a highly variable relationship between depth and damage. However, while Wing *et al.* demonstrated low skill at the property level, when results were aggregated the local biases generally cancelled each other out. Since this study focuses on large-scale flood risk, rather than that of individual locations, this inventory of residential and non-residential functions is a suitable (and the only) choice.

For this analysis, the central tendencies of the damage functions were leveraged deterministically. The curves were then input into an open-source consequence engine developed by USACE called go-consequences (see Code Availability). Damages were computed for the 2-, 5-, 20-, 100-, 250-, and 500-year return periods, which were then integrated using trapezoidal Riemann sums to compute an AAL for each location. Two important assumptions were adopted. Firstly, no damages were accrued between the most frequent damage and the annual flood (100% annual exceedance probability) when integrating. If damages did not occur until the 100-year flood, no damages would be assumed until that frequency. The second is that for the space between the 500-year and the ∞-year (0% annual exceedance probability) frequency damage, the value of the 500-year damage was used as the maximum allowable damage (i.e. no extrapolation). Both of these assumptions tend to reduce the estimated damages, so our estimates should yield a conservative deterministic estimate. These are both standard assumptions in flood risk estimation, but are important to state as alternatives used in their place tend to dramatically overstate risk.

Census tract data

Demographic data split by census tract were obtained from the 2019 American Community Survey 5-year rollup. The proportion of census tract populations which fell into a specific socio-economic grouping was computed by dividing the counts of each group by the total census tract population. The groups examined were: (i) below 100% of the poverty level (B06012_002), (ii) not Hispanic or Latino, White alone (B03002_003), (iii) not Hispanic or Latino, Black or African American alone (B03002_004), (iv) Hispanic or Latino (B03002_012), (v) not Hispanic or Latino, American Indian and Alaska Native alone (B03002_006), and (vi) other racial identities which do not fall into the groups mentioned here (ii-v) were combined into an ‘other’ group, calculated from the remaining census tract population yet to be allocated a group (B01001_001).

Declarations

Data Availability

The flood hazard data used in this analysis is available from Bates et al. (2021), with details on constituent data availability contained therein. Alternatively, the data can be viewed at https://floodfactor.com/. The building data used in this analysis is currently restricted from public use. Vulnerability functions (and the code for computation of losses) are available at https://github.com/USACE/go-consequences. EPA EnviroAtlas and ICLUS population data are available from https://edg.epa.gov/. The R package tidycensus (https://cran.r-project.org/package=tidycensus) was used to obtain data from the American Community Survey.

Code Availability

The loss calculations were made using the go-consequences codebase, available at https://github.com/USACE/go-consequences and published under the MIT license. A freely available version of the underlying computational hydraulic engine, LISFLOOD-FP 8.0, is available from https://zenodo.org/record/4073011#.YFCo8Wj7SUl.

Acknowledgements

The authors are grateful to N. B. Kalman of University of California, Davis for assisting with the NFIP data analysis. Paul Bates was supported by a Royal Society Wolfson Research Merit Award. Research in this paper was in part supported by UK Natural Environment Research Council grant NE/V017756/1.

Author Contributions

O.E.J.W., P.D.B., C.C.S., N.Q., A.M.S., and J.C.N. conceived the project. C.C.S., N.Q., and A.M.S. developed the flood model. W.L. developed and ran the consequences engine. O.E.J.W. performed all analyses. O.E.J.W. wrote the manuscript. All authors aided in the refinement, interpretation, and discussion of the analyses.

Competing Interests

The authors declare no competing interests.

Additional Information

Supplementary Information is available for this paper. Correspondence and requests for materials should be addressed to Oliver Wing (o.wing@fathom.global). Reprints and permissions information is available at www.nature.com/reprints.

References

1. Trenberth, K. E., Dai, A., Rasmussen, R. M. & Parsons, D. B. The changing character of precipitation. *Bull. Am. Meteorol. Soc.* **84**, 1205–1218 (2003).
2. Kundzewicz, Z. W. et al. Flood risk and climate change: global and regional perspectives. *Hydrol. Sci. J.* **59**, 1–28 (2014).
3. Markonis, Y., Papalexiou, S. M., Martinkova, M. & Hanel, M. Assessment of water cycle intensification over land using a multisource global gridded precipitation dataset. *J. Geophys. Res. Atmos.* **124**, 11175–11187 (2019).
4. Gudmundsson, L. et al. Globally observed trends in mean and extreme river flow attributed to climate change. *Science* **371**, 1159–1162 (2021).
5. Kopp, R. E. et al. Probabilistic 21st and 22nd century sea-level projections at a global network of tide-gauge sites. *Earth's Future* **2**, 383–406 (2014).
6. Oppenheimer, M. et al. Sea level rise and implications for low-lying islands, coasts and communities. In: *IPCC Special Report on the Ocean and Cryosphere in a Changing Climate* (IPCC, 2019).
7. Marsooli, R., Lin, N., Emanuel, K. & Feng, K. Climate change exacerbates hurricane flood hazards along US Atlantic and Gulf Coasts in spatially varying patterns. *Nat. Commun.* **10**, 3785 (2019).
8. IPCC. *Global Warming of 1.5°C. An IPCC Special Report on the impacts of global warming of 1.5°C above pre-industrial levels and related global greenhouse gas emission pathways, in the context of strengthening the global response to the threat of climate change, sustainable development, and efforts to eradicate poverty* (IPCC, 2018).
9. Ward, P. J. et al. Assessing flood risk at the global scale: model setup, results, and sensitivity. *Environ. Res. Lett.* **8**, 044019 (2013).
10. Alfieri, L. et al. Global projections of river flood risk in a warmer world. *Earth's Future* **5**, 171–182 (2017).
11. Hirabayashi, Y. et al. Global flood risk under climate change. *Nat. Clim. Chang.* **3**, 816–821 (2013).
12. Winsemius, H. C. et al. Global drivers of future river flood risk. *Nat. Clim. Chang.* **6**, 381–385 (2016).
13. Kulp, S. A. & Strauss, B. H. New elevation data triple estimates of global vulnerability to sea-level rise and coastal flooding. *Nat. Commun.* **10**, 4844 (2019).
14. Scussolini, P. et al. FLOPROS: an evolving global database of flood protection standards. *Nat. Hazards Earth Syst. Sci.* **16**, 1049–1061 (2016).
15. Wing, O. E. J. et al. A new automated method for improved flood defense representation in large-scale hydraulic models. *Water Resour. Res.* **55**, 11007–11034 (2019).
16. Emanuel, K. A. Downscaling CMIP5 climate models shows increased tropical cyclone activity over the 21st century. *Proc. Natl. Acad. Sci. U.S.A.* **110**, 347–368 (2013).
17. Kendon, E. J. et al. Heavier summer downpours with climate change revealed by weather forecast resolution model. *Nat. Clim. Chang.* **4**, 570–576 (2014).
18. Dottori, F. et al. Development and evaluation of a framework for global flood hazard mapping. *Adv. Water Resour.* **94**, 87–102 (2016).

19. Ward, P. J. et al. A global framework for future costs and benefits of river-flood protection in urban areas. *Nat. Clim. Chang.* **7**, 642–646 (2017).
20. Wing, O. E. J. et al. Validation of a 30 m resolution flood hazard model of the conterminous United States. *Water Resour. Res.* **53**, 7968–7986 (2017).
21. Association of State Floodplain Managers. *Flood Mapping for the Nation: A Cost Analysis for Completing and Maintaining the Nation's NFIP Flood Map Inventory*. (Association of State Floodplain Managers, 2020).
22. U.S. Water Resources Council. *Economic and Environmental Principles and Guidelines for Water and Related Land Resources Implementation Studies*. (U.S. Water Resources Council, 1983).
23. Bates, P. D. et al. Combined modeling of US fluvial, pluvial, and coastal flood hazard under current and future climates. *Water Resour. Res.* **57**, WR028673 (2021).
24. Wing, O. E. J. et al. Simulated historical flood events at the continental scale: observational validation of a large-scale hydrodynamic model. *Nat. Hazards Earth Syst. Sci.* **21**, 559–575 (2021).
25. Ting, M., Kossin, J. P., Camargo, S. J. & Li, C. Past and future hurricane intensity change along the U.S. east coast. *Sci. Rep.* **9**, 7795 (2019).
26. Kousky, C. Financing flood losses: a discussion of the National Flood Insurance Program. *Risk Manag. Insur. Rev.* **21**, 11–32 (2018).
27. Blessing, R. A., Sebastian, A. & Brody, S. D. Flood risk delineation in the United States: how much loss are we capturing? *Nat. Hazards Rev.* **18**, 04017002 (2017).
28. Wing, O. E. J. et al. Estimates of present and future flood risk in the conterminous United States. *Environ. res. Lett.* **13**, 034023 (2018).
29. Kousky, C. & Golnaraghi, M. *Flood Risk Management in the United States: Building Flood Resilience in a Changing Climate*. (Geneva Association, 2020).
30. FEMA. *National Advisory Council Report to the FEMA Administrator*. (FEMA, 2020).
31. Billings, S. B., Gallagher, E. & Ricketts, L. *Let the Rich Be Flooded: The Distribution of Financial Aid and Distress after Hurricane Harvey.* (SSRN, 2019).
32. Pralle, S. Drawing lines: FEMA and the politics of mapping flood zones. *Clim. Change* **152**, 227–237 (2019).

32. Sampson, C. C. et al. A high-resolution global flood hazard model. *Water Resour. Res.* **51**, 7358–7381 (2015).
33. Bates, P. D., Horritt, M. S. & Fewtrell, T. J. A simple inertial formulation of the shallow water equations for efficient two-dimensional flood inundation modeling. *J. Hydrol.* **236**, 54–77 (2010).
34. Neal, J., Schumann, G. & Bates, P. A subgrid channel model for simulating river hydraulics and floodplain inundation over large and data sparse areas. *Water Resour. Res.* **48**, WR012514 (2012).
35. de Almeida, G. A. M. & Bates, P. Applicability of the local inertial approximation of the shallow water equations to flood modeling. *Water Resour. Res.* **49**, 4833–4844 (2013).

36. Hunter, N. M., Horritt, M. S., Bates, P. D., Wilson, M. D. & Werner, M. G. F. An adaptive time step solution for raster-based storage cell modelling of floodplain inundation. *Adv. Water Resour.* **28**, 975–991 (2005).
37. Neal, J., Dunne, T., Sampson, C., Smith, A. & Bates, P. Optimisation of the two-dimensional hydraulic model LISFLOOD-FP for CPU architecture. *Environ. Model. Softw.* **107**, 148–157 (2018).
38. Neal, J. et al. Representation of river channels in large scale flood inundation models. *Water Resour. Res.* (under review)
39. Smith, A., Sampson, C. & Bates, P. Regional flood frequency analysis at the global scale. *Water Resour. Res.* **51**, 539–553 (2015).
40. McMillan, H., Krueger, T. & Freer, J. Benchmarking observational uncertainties for hydrology: rainfall, river discharge and water quality. *Hydrol. Process.* **26**, 4078-4111 (2012).
41. Emanuel, K., Sundararajan, R. & Williams, J. Hurricanes and global warming: results from downscaling IPCC AR4 simulations. *Bull. Am. Meteorol. Soc.* **89**, 347–368 (2008).
42. Feldmann, M., Emanuel, K., Zhu, L. & Lohmann, U. Estimation of Atlantic tropical cyclone rainfall frequency in the United States. *J. Appl. Meteorol. Climatol.* **58**, 1853–1866 (2019).
43. Muis, S., Verlaan, M., Winsemius, H. C., Aerts, J. C. J. H. & Ward, P. J. A global reanalysis of storm surges and extreme sea levels. *Nat. Commun.* **7**, 11969 (2016).
44. Mandli, K. T. & Dawson, C. N. Adaptive mesh refinement for storm surge. *Ocean Model.* **75**, 36–50 (2014).
45. Quinn, N. et al. The spatial dependence of flood hazard and risk in the United States. *Water Resour. Res.* **55**, 1890–1911 (2019).
46. U.S. Army Corps of Engineers Hydrologic Engineering Center. NSI Technical Documentation. https://www.hec.usace.army.mil/confluence/nsidocs/nsi-technical-documentation-50495938.html (2021).
47. U.S. Environmental Protection Agency. *Updates to the Demographic and Spatial Allocation Models to Produce Integrated Climate and Land Use Scenarios (ICLUS) Version 2*. (National Center for Environmental Assessment, 2016).
48. U.S. Army Corps of Engineers. *Economic Guidance Memorandum 01-03, Generic Depth-Damage Relationships for Residential Structures Without Basements*. (USACE, 2000).
49. U.S. Army Corps of Engineers. *Economic Guidance Memorandum 04-01, Generic Depth-Damage Relationships for Residential Structures With Basements*. (USACE, 2003).
50. Scawthorn, C. et al. HAZUS-MH flood loss estimation methodology. II. Damage and loss assessment. *Nat. Hazards Rev.* **7**, 72–81 (2006).
51. Wing, O. E. J., Pinter, N., Bates, P. D. & Kousky, C. New insights into flood vulnerability revealed from flood insurance big data. *Nat. Commun.* **11**, 1444 (2020).

Figures

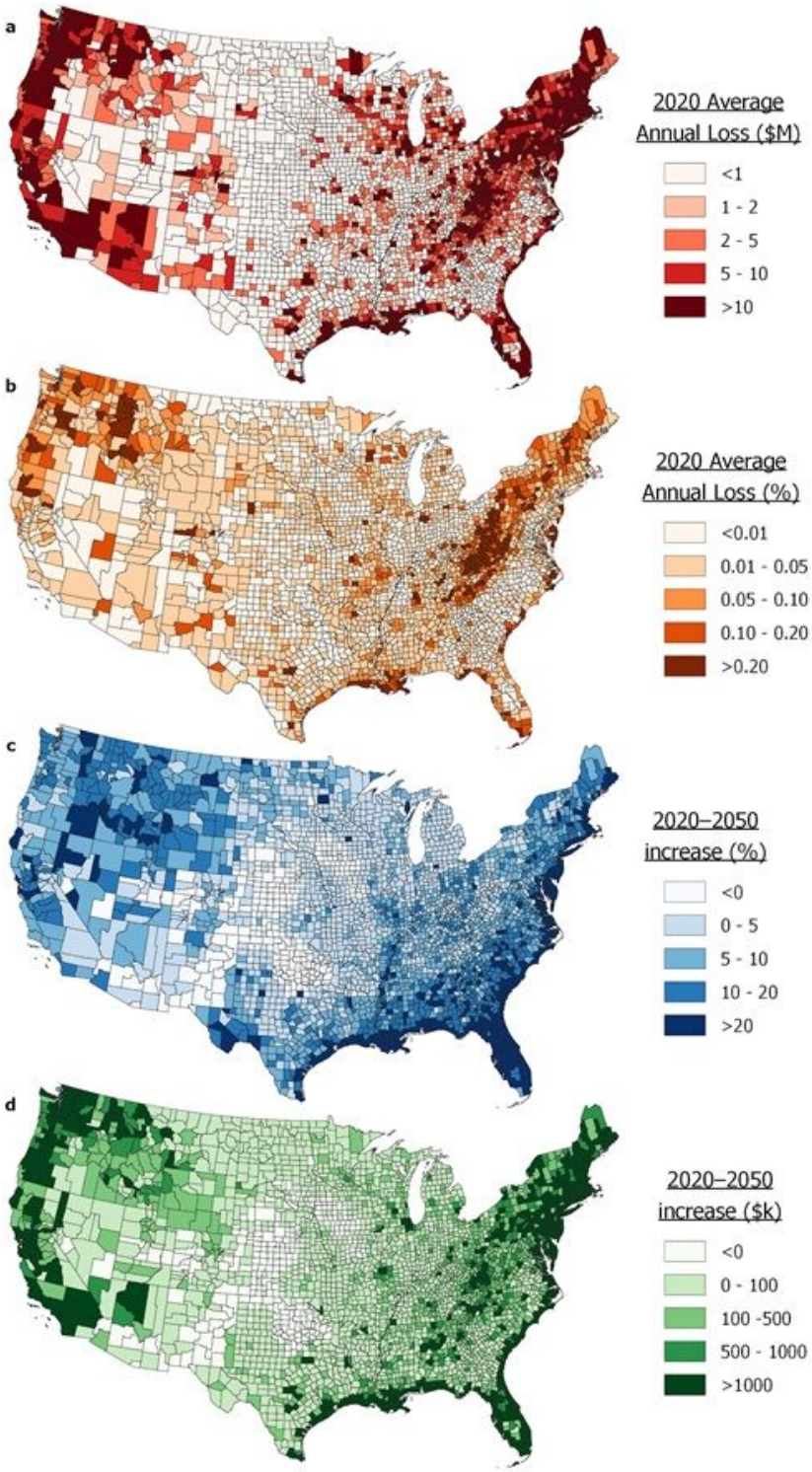

Figure 1

Present and future U.S. flood risk by county. a Absolute average annual loss (AAL) in 2020. b Relative AAL in 2020. c Relative AAL increase by 2050. d Absolute AAL increase by 2050.

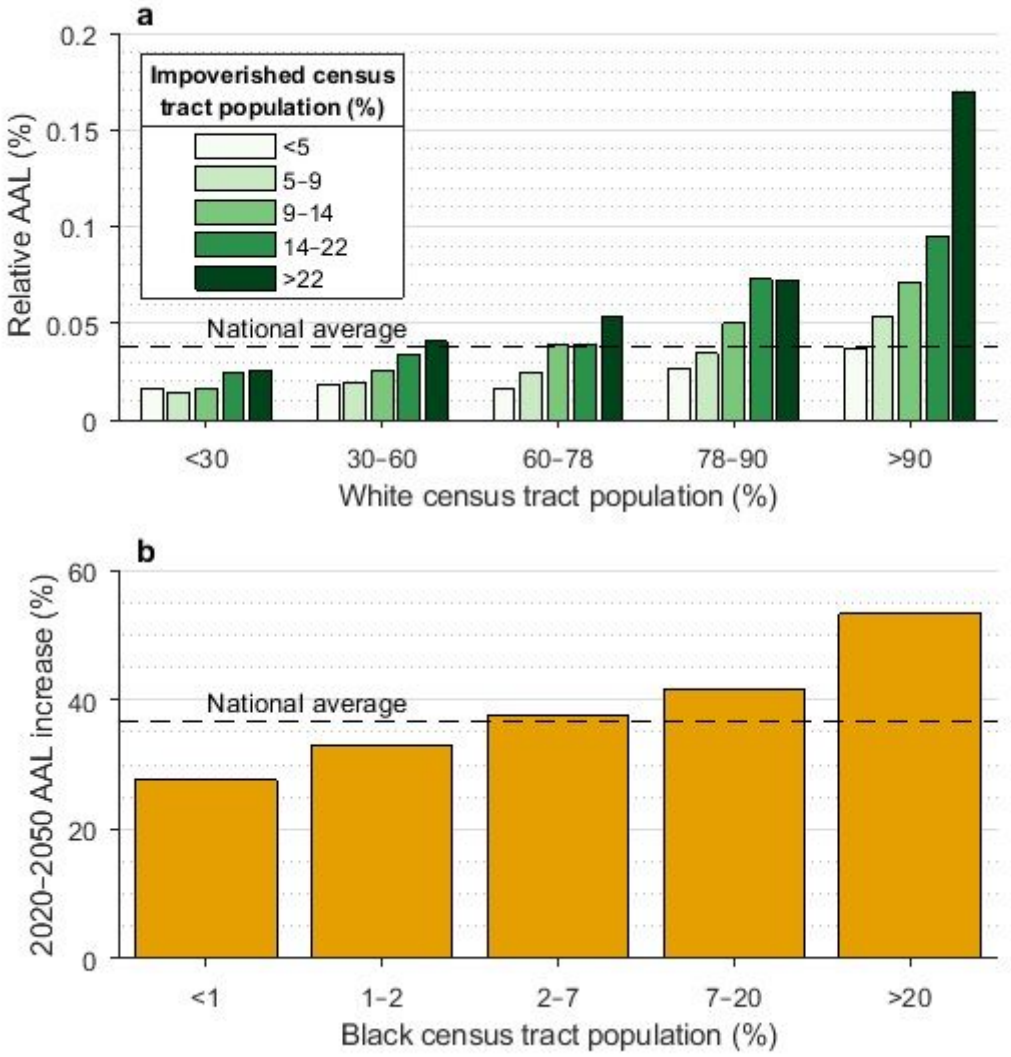

Figure 2

Relative U.S. flood risk for different demographics groups. a Annual average loss (AAL) as a proportion of exposure summarised for census tract quintile bins of White population proportion, further broken down by quintile of population proportion in poverty. b AAL increase from 2020 to 2050 for census tract quintile bins of Black population proportion.

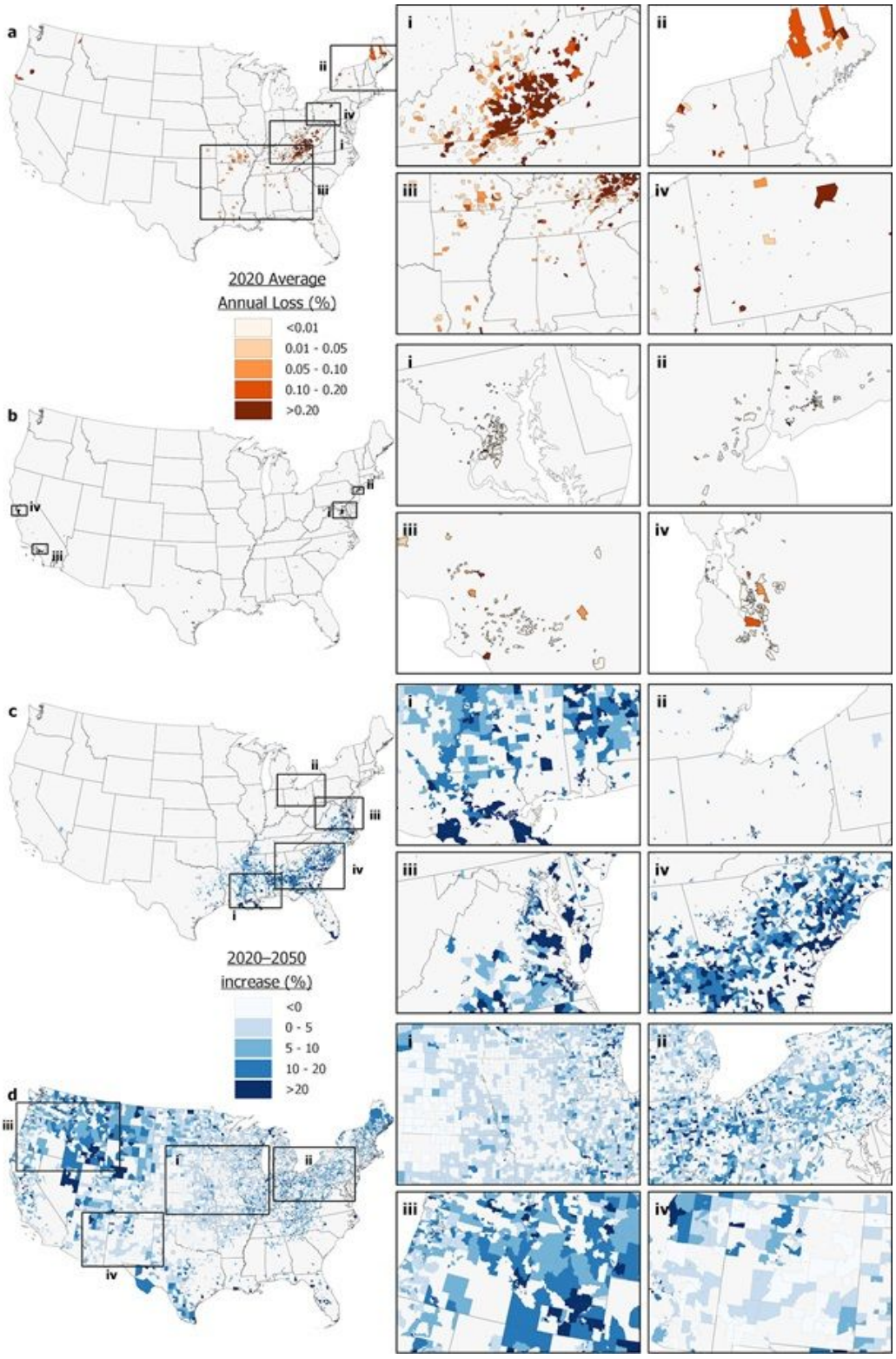

Figure 3

Present and future spatial distribution of flood risk amongst select demographic groups. a Relative flood risk of census tracts which fall into the top 20% White population proportion and top 20% poverty rate. b Relative flood risk of census tracts which fall into the bottom 20% White population proportion and bottom 20% poverty rate. c Relative flood risk increase to 2050 of census tracts in the top 20% Black

population proportion. d Relative flood risk increase to 2050 of census tracts in the bottom 20% Black population proportion. Panels i-iv highlight selected areas for each panel a-d.

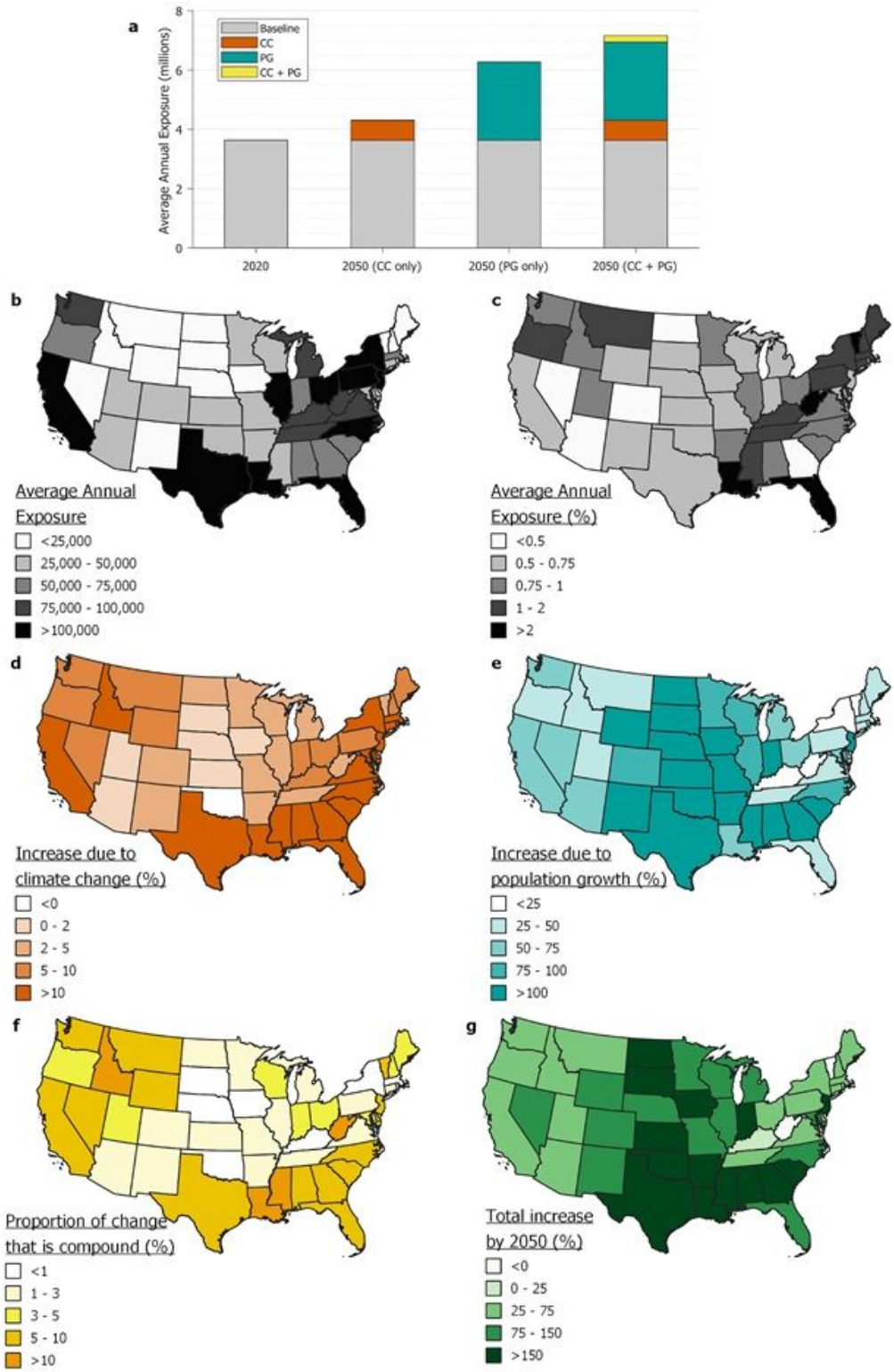

Figure 4

The impact of climate change and population growth on future U.S. flood risk by state. a Nationwide average annual exposure (AAE) of the present and future broken down into its constituent drivers. b Absolute AAE in 2020. c Relative AAE in 2020. d AAE increase from 2020 to 2050 from climate change

alone. e AAE increase from 2020 to 2050 from population growth alone. f AAE increase from 2020 to 2050 from only the compound effects of climate change and population growth. g AAE increase from 2020 to 2050.

Supplementary Files

This is a list of supplementary files associated with this preprint. Click to download.

- WingetalSIsubmitted.docx